Densities and Shear Viscosities of Anisole with Nitrobenzene, Chlorobenzene, Carbon Tetrachloride, 1,2-Dichloroethane, and Cyclohexane from 25 to 40 °C

Shrikant S. Joshi and Tejraj M. Aminabhavi*,†

Department of Chemistry, Karnatak University, Dharwad 580003, India

Shyam S. Shukla

Department of Chemistry, Lamar University, P.O. Box 10022, Beaumont, Texas 77710

Results of density and shear viscosity for the binaries of anisole with nitrobenzene, chlorobenzene, carbon tetrachloride, cyclohexane, and 1,2-dichloroethane have been used to estimate the excess volume, excess shear viscosity, excess free energy of activation of flow, partial molar volume, contact parameter, and density increment over the entire mixture composition. A temperature variation of shear viscosity was used to estimate the enthalpy, $\Delta H^{\ddagger}$, and entropy, $\Delta S^{\ddagger}$, of activation for the flow process. The calculated quantities have been discussed in terms of the type and nature of thermodynamic interactions between the mixing components. Furthermore, attempts have been made to test the relative validity of the viscosity models proposed by McAllister, Heric, and Auslaender.

Introduction

In continuation of our ongoing research program (*1-3*) concerning the thermodynamic interactions in binary mixtures, we now present some binary data on densities and shear viscosities of five mixtures of anisole with nitrobenzene, chlorobenzene, carbon tetrachloride, 1,2-dichloroethane (DCE), or cyclohexane at 25, 30, 35, and 40 °C. These results are employed in the computation of excess parameters such as excess volume, V^E, excess viscosity, η^E, and excess free energy of activation of flow, G^E, in addition to partial molar volumes, $\bar{V}_1$ and $\bar{V}_2$, of the components 1 and 2, respectively. The enthalpy, $\Delta H^{\ddagger}$ and entropy, $\Delta S^{\ddagger}$ of activation of flow have been obtained from the temperature variation of mixture viscosity. Calculated results are discussed in terms of the nature of interacting molecules of the mixture. Binary viscosity data are also used to test the validity of viscosity theories of the three-body interaction model of McAllister (*4*), Heric (*5*, *6*), and Auslaender (*7*).

Experimental Section

The solvents used in this research were obtained in their highest purity and further purified by the procedures described elsewhere (*8*). Binary mixtures were prepared by accurately weighing the liquids in specially designed stoppered bottles. Density, ρ, and viscosity, η, measurements were made by using a pycnometer and a Cannon-Fenske viscometer (size 100), respectively; these procedures have been described earlier (*9*). An average of the triplicate measurements of ρ and η were used in the calculation of thermodynamic quantities. The possible errors in the measurement of ρ and η are respectively 0.0002 and 0.0008 unit.

† Also adjunct research professor of chemistry, Lamar University.

Table I. Comparison of Physical Properties of Pure Liquids with Literature at 25 °C

liquid	boiling point, °C		density, g·cm^{-3}	
	obsd	lit.[a]	obsd	lit.[a]
anisole	154.0	153.8	0.989 46	0.989 32
cyclohexane	81.0	80.7	0.773 73	0.773 89
nitrobenzene	211.0	210.8	1.198 50	1.198 35
chlorobenzene	132.0	131.7	1.095 51[b]	1.095 50[b]
1,2-dichloroethane	84.0	83.5	1.245 52	1.245 80
carbon tetrachloride	77.0	76.8	1.574 90[b]	1.574 80[b]

[a] Reference 8. [b] These values at 30 °C.

Theoretical Relations and Data Treatment

Table I lists pure-component data that compare well with the literature (*8*). The experimental ρ and η of the five binary mixtures at four temperatures are given in Table II. These data have been used to calculate the excess molar volume, excess molar shear viscosity, and excess molar Gibbs free energy of activation of flow by the use of the following relations

$$V^E\ (\mathrm{cm^3/mol}) = V_m - V_1x_1 - V_2x_2 \quad (1)$$

$$\eta^E\ (\mathrm{cP}) = \eta - \eta_1x_1 - \eta_2x_2 \quad (2)$$

$$G^E\ (\mathrm{kcal/mol}) = RT[\ln(\eta V_m) - x_1 \ln(\eta_1 V_1) - x_2 \ln(\eta_2 V_2)] \quad (3)$$

where V_1, V_2, and V_m represent respectively the molar volumes of components 1 and 2 and their mixture and η_1 and η_2 are the viscosities and x_1 and x_2 represent the mole fractions of components 1 and 2, respectively. The term, RT, has the conventional meaning.

The partial molar volumes, $\bar{V}_1$ and $\bar{V}_2$, of components 1 and 2 have been calculated with use of the relations

$$\bar{V}_1\ (\mathrm{cm^3/mol}) = V_1 + V^E/x_1 + x_1x_2[\partial(V^E/x_1)/\partial x_1] \quad (4)$$

$$\bar{V}_2\ (\mathrm{cm^3/mol}) = V_2 + V^E/x_2 + x_1x_2[\partial(V^E/x_2)/\partial x_2] \quad (5)$$

Each of the above sets of results has been fitted to

$$Y = x_1x_2\sum_{i=1}^{4} a_i(x_2 - x_1)^{i-1} \quad (6)$$

to evaluate the coefficients, a_i. Here, Y refers to V^E, η^E, G^E, $\bar{V}_1$, or $\bar{V}_2$.

A nonlinear regression analysis based on the Marquardt algorithm was used with a 640K PC to estimate the coefficients. In each case, the optimum number of coefficients was ascertained from an examination of the variation in standard error, σ, as given by

$$\sigma = [\sum(Y_{obs} - Y_{cal})^2/(n - p)]^{1/2} \quad (7)$$

where p is the number of parameters (four, viz., a_1, a_2, a_3, and

0021-9568/90/1735-0247$02.50/0

Table II. Densities (ρ) and Viscosities (η) of Binary Mixtures at Various Temperatures

	ρ, g·cm^{-3}				η, cP			
x_1	25 °C	30 °C	35 °C	40 °C	25 °C	30 °C	35 °C	40 °C
				(A) Anisole (1)–Cyclohexane (2)				
0.0	0.7737	0.7686	0.7640	0.7594	0.8876	0.8192	0.7546	0.6934
0.1016	0.7932	0.7883	0.7838	0.7788	0.8187	0.7586	0.7009	0.6496
0.1993	0.8131	0.8080	0.8032	0.7986	0.7856	0.7308	0.6800	0.6314
0.3005	0.8335	0.8288	0.8248	0.8190	0.7700	0.7174	0.6680	0.6223
0.3997	0.8551	0.8496	0.8448	0.8402	0.7696	0.7169	0.6674	0.6228
0.5014	0.8767	0.8715	0.8671	0.8622	0.7849	0.7317	0.6829	0.6370
0.6014	0.8988	0.8939	0.8889	0.8842	0.8030	0.7509	0.7001	0.6546
0.7043	0.9196	0.9167	0.9121	0.9075	0.8378	0.7843	0.7318	0.6823
0.8000	0.9436	0.9388	0.9342	0.9290	0.8834	0.8216	0.7693	0.7163
0.8992	0.9661	0.9613	0.9563	0.9515	0.9338	0.8700	0.8092	0.7511
1.0000	0.9895	0.9842	0.9796	0.9750	0.9785	0.9070	0.8422	0.7814
				(B) Anisole (1)–Nitrobenzene (2)				
0.0	1.1985	1.1932	1.1880	1.1832	1.8172	1.6662	1.5281	1.4022
0.1000	1.1716	1.1666	1.1623	1.6923	1.5560	1.4301	1.3171	1.3171
0.2022	1.1546	1.1496	1.1444	1.1397	1.5607	1.4434	1.3262	1.2240
0.3039	1.1334	1.1281	1.1232	1.1180	1.4540	1.3388	1.2359	1.1416
0.3968	1.1136	1.1086	1.1034	1.0987	1.3679	1.2626	1.1647	1.0783
0.5018	1.0915	1.0865	1.0817	1.0765	1.2811	1.1863	1.0963	1.0132
0.6021	1.0708	1.0653	1.0604	1.0559	1.2039	1.1151	1.0308	0.9572
0.7032	1.0499	1.0449	1.0399	1.0352	1.1464	1.0641	0.9838	0.9119
0.8267	1.0243	1.0196	1.0149	1.0100	1.0685	0.9924	0.9200	0.8533
0.9043	1.0086	1.0037	0.9987	0.9941	1.0453	0.9678	0.8978	0.8343
1.0	0.9895	0.9842	0.9796	0.9750	0.9785	0.9070	0.8422	0.7814
				(C) Anisole (1)–1,2-Dichloroethane (2)				
0.0	1.2455	1.2382	1.2304	1.2234	0.7833	0.7400	0.6929	0.6523
0.0971	1.2112	1.2044	1.1968	1.1901	0.8095	0.7615	0.7135	0.6712
0.1961	1.1790	1.1721	1.1655	1.1588	0.8125	0.7644	0.7190	0.6736
0.2958	1.1495	1.1427	1.1365	1.1300	0.8228	0.7712	0.7246	0.6785
0.3963	1.1218	1.1151	1.1098	1.1029	0.8354	0.7823	0.7333	0.6881
0.4918	1.0970	1.0908	1.0850	1.0790	0.8519	0.7983	0.7466	0.7004
0.5946	1.0721	1.0662	1.0606	1.0552	0.8754	0.8183	0.7639	0.7150
0.6933	1.0500	1.0446	1.0390	1.0337	0.9012	0.8399	0.7821	0.7319
0.7944	1.0288	1.0232	1.0181	1.0132	0.9299	0.8693	0.8076	0.7519
0.8972	1.0085	1.0032	0.9980	0.9931	0.9672	0.8983	0.8340	0.7759
1.0	0.9895	0.9842	0.9796	0.9750	0.9785	0.9070	0.8422	0.7814
				(D) Anisole (1)–Chlorobenzene (2)				
0.0	1.1010	1.0955	1.0897	1.0844	0.7562	0.7155	0.6769	0.6370
0.0994	1.0893	1.0838	1.0780	1.0728	0.7921	0.7495	0.7047	0.6642
0.2000	1.0776	1.0719	1.0663	1.0609	0.8143	0.7657	0.7212	0.6768
0.2957	1.0663	1.0608	1.0557	1.0503	0.8336	0.7850	0.7354	0.6921
0.3982	1.0548	1.0491	1.0441	1.0388	0.8576	0.8026	0.7535	0.7064
0.5028	1.0431	1.0375	1.0324	1.0283	0.8800	0.8232	0.7693	0.7227
0.6002	1.0321	1.0272	1.0218	1.0170	0.9024	0.8438	0.7866	0.7366
0.7006	1.0214	1.0159	1.0108	1.0059	0.9275	0.8635	0.8038	0.7511
0.7995	1.0104	1.0054	1.0005	0.9955	0.9474	0.8808	0.8201	0.7649
0.8997	1.0003	0.9951	0.9903	0.9858	0.9779	0.9091	0.8444	0.7855
1.0	0.9895	0.9842	0.9796	0.9750	0.9785	0.9070	0.8422	0.7814
				(E) Anisole (1)–Carbon Tetrachloride (2)				
0.0	1.5851	1.5749	1.5650	1.5554	0.9275	0.8702	0.8162	0.7676
0.1050	1.5157	1.5062	1.4970	1.4882	0.9408	0.8895	0.8268	0.7762
0.2013	1.4537	1.4450	1.4362	1.4275	0.9425	0.8842	0.8263	0.7751
0.3026	1.3899	1.3815	1.3734	1.3658	0.9493	0.8852	0.8279	0.7851
0.3956	1.3329	1.3254	1.3176	1.3105	0.9547	0.8927	0.8326	0.7777
0.5023	1.2691	1.2617	1.2546	1.2478	0.9644	0.9013	0.8397	0.7837
0.5968	1.2133	1.2066	1.1938	1.1934	0.9745	0.9054	0.8446	0.7864
0.6990	1.1547	1.1486	1.1423	1.1364	0.9834	0.9147	0.8502	0.7919
0.7970	1.1001	1.0946	1.0883	1.0831	0.9896	0.9190	0.8547	0.7946
0.8998	1.0433	1.0378	1.0325	1.0276	0.9961	0.9260	0.8580	0.7981
1.0	0.9895	0.9842	0.9796	0.9750	0.9785	0.9070	0.8422	0.7814

a_4) and n is the number of data points (usually eleven). Computation of V^E, η^E, and G^E from eqs 1–3 is straightforward. However, to compute the experimental values of $\bar{V}_1$ and $\bar{V}_2$, the needed derivatives, viz., $\partial(V^E/x_1)/\partial x_1$ and $\partial(V^E/x_2)/\partial x_2$, of eqs 4 and 5 were obtained from a differentiation of the computed V^E from eq 6. Values of the estimated coefficients together with the standard errors as obtained from eq 7 are given in Table III.

Following our earlier suggestions (*10*, *11*), the Flory–Scatchard-type contact interaction parameter, A_{12}, and the associated density increment, $(\partial\rho/\partial\phi_1)_{P,T}$, are computed by using eqs 8 and 9, where $\phi_i (\equiv x_1V_1/\sum_{i=1}^{2} x_iV_i)$ represents the volume fraction of the ith component of the mixture. Results of eqs 8 and 9 have been subjected to computer analysis to

$$A_{12} = (\phi_1\rho_1 + \phi_2\rho_2 - \rho)/\phi_1\phi_2\rho \quad (8)$$

$$(\partial\rho/\partial\phi_1)_{P,T} = \frac{(\rho_1 - \rho_2) - \rho[A_{12}(\phi_2 - \phi_1) + (dA_{12}/d\phi_1)(\phi_1\phi_2)]}{1 + A_{12}\phi_1\phi_2} \quad (9)$$

derive the coefficients, a_i, from eq 10. Here, Y refers to A_{12} or $(\partial\rho/\partial\phi_1)_{P,T}$; these results are also included in Table III.

$$Y = a_1 + a_2(\phi_2 - \phi_1) + a_3(\phi_2 - \phi_1)^2 \qquad (10)$$

An increase in temperature decreases the shear viscosity of the medium. This observation (*12*) has led us to compute the thermodynamic quantities, viz., enthalpy, $\Delta H^{\ddagger}$, and entropy of flow, $\Delta S^{\ddagger}$, as

$$\ln(\lambda V) = \ln(hN) - \Delta S^{\ddagger}/R + (\Delta H^{\ddagger}/R)\frac{1}{T} \qquad (11)$$

where λ ($\equiv\eta/\rho$) is kinematic viscosity, h is Planck's constant, and N is the Avogadro number. From a least-squares analysis, $\Delta H^{\ddagger}$ and $\Delta S^{\ddagger}$ have been estimated.

The kinematic viscosities were also used to test the validity of McAllister's three-body model (*4*) and Heric's relations (*5*, *6*).

$$\ln\lambda = x_1^3 \ln\lambda_1 + 3x_1^2 x_2 \ln a + 3x_1x_2^2 \ln b + x_2^3 \ln\lambda_2 - \ln[x_1 + x_2M_2/M_1] + 3x_1^2x_2 \ln[(2 + M_2/M_1)/3] + 3x_1x_2^2 \ln[(1 + 2M_2/M_1)/3] + x_2^3 \ln(M_2/M_1) \qquad (12)$$

$$\lambda = x_1\lambda_1 + x_2\lambda_2 + x_1x_2[a + b(x_2 - x_1) + c(x_2 - x_1)^2] \qquad (13)$$

$$\ln\lambda = x_1 \ln\lambda_1 + x_2 \ln\lambda_2 + x_1 \ln M_1 + x_2 \ln M_2 - \ln(x_1M_1 + x_2M_2) + x_1x_2[a + b(x_2 - x_1) + c(x_2 - x_1)^2] \qquad (14)$$

The Auslaender relation (*7*) for the absolute viscosity of the mixture is given as

$$x_1(x_1 + ax_2)(\eta - \eta_1) + bx_2(cx_1 + x_2)(\eta - \eta_2) = 0 \qquad (15)$$

The coefficients a, b, and c in all the viscosity models have been estimated from the least-squares method. These models are used to predict binary viscosities; while doing so, the standard error involved in the predicted and measured viscosities will indicate the extent of validity of the viscosity model.

Discussion

Density results of all the mixtures at 25 °C are given in Figure 1. For mixtures of anisole with carbon tetrachloride or 1,2-dichloroethane, the ρ versus x_1 plots are slightly curved whereas, with cyclohexane, chlorobenzene, or nitrobenzene mixtures, the linear dependencies are observed. Viscosity behavior of all the mixtures at 25 °C is presented in Figure 2, wherein mixtures of anisole with cyclohexane or nitrobenzene exhibit somewhat greater deviations from the linear behavior as compared to other mixtures.

Excess molar volume versus mole fraction of the first component as shown in Figure 3 is negative for mixtures of anisole with nitrobenzene or carbon tetrachloride, whereas it is positive for mixtures of anisole with cyclohexane or DCE. In the case of mixtures of anisole with cyclohexane, V^E (=0.743 cm^3/mol) is the largest and positive among the liquids considered; this suggests the presence of weak dispersion interactions between the molecules. This is also supported by the fact that the molar volume of anisole (V_1 = 109.3 cm^3/mol) is quite close to that of cyclohexane (V_2 = 108.8 cm^3/mol). The largest negative V^E as seen in the case of the anisole (1)–nitrobenzene (2) system is attributed to specific interactions due to an induced dipole effect (μ of nitrobenzene at 25 °C is 4.03 D, and for anisole it is 1.245 D) (*8*). Additionally, large differences in their dielectric constants (ϵ of nitrobenzene is 34.82 at 25 °C, and for anisole it is 4.33 at 25 °C) might be responsible for the considerable specific interactions between the mixing components, leading to large negative V^E (V^E_{max} = −0.119 cm^3/mol). Similarly, carbon tetrachloride (with zero dipole moment) when mixed with anisole yields small but negative V^E (V^E_{max} = −0.066 cm^3/mol). However, for the anisole (1)–chlorobenzene (2) system, both positive and negative V^E values are observed, and these lie in the neighborhood of the zero scale, (see Figure 3).

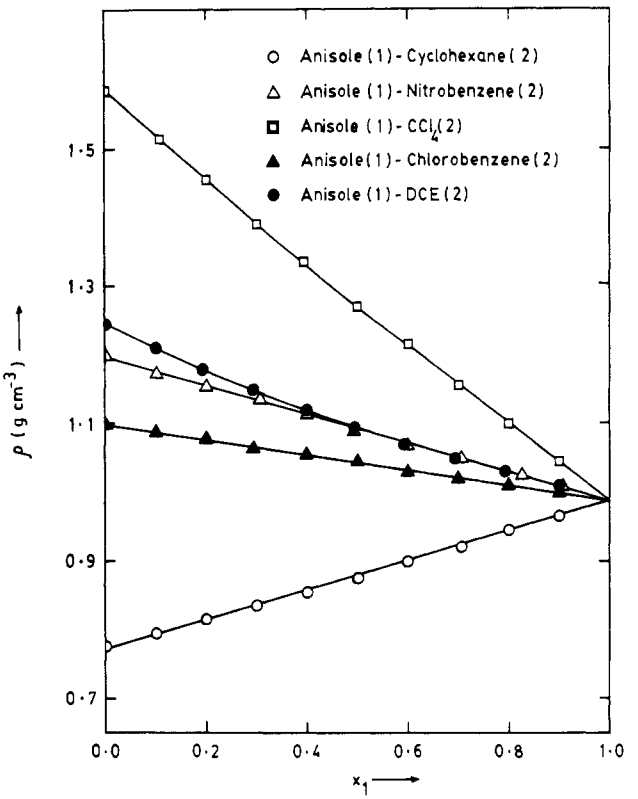

Figure 1. Dependence of density on mole fraction at 25 °C. Symbols: for binaries of anisole with (○) cyclohexane; (△) nitrobenzene; (□) carbon tetrachloride; (●) 1,2-dichloroethane; (▲) chlorobenzene.

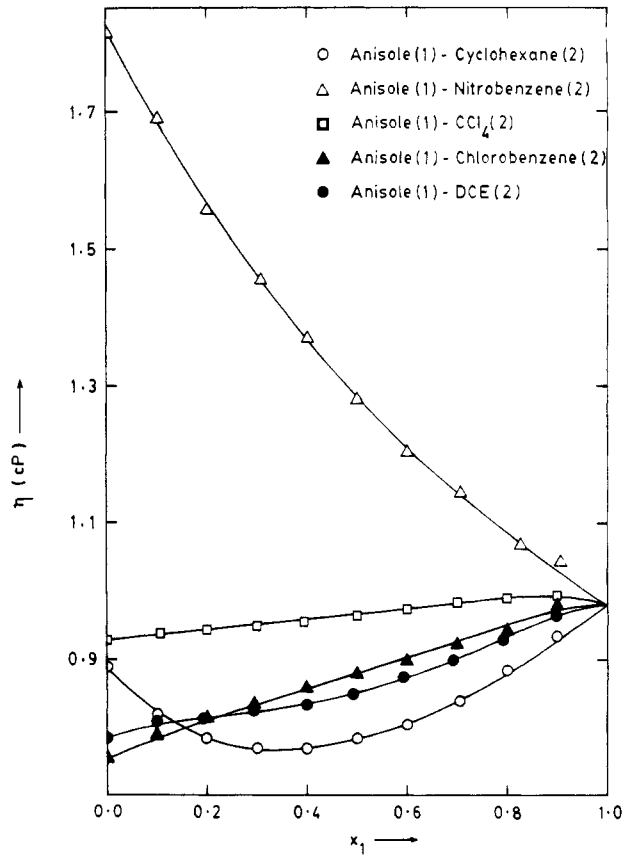

Figure 2. Dependence of viscosity on mole fraction at 25 °C. Symbols have the same meaning as in Figure 1.

Table III. Estimated Parameters of Various Functions

function	temp, °C	a_1	a_2	a_3	a_4	σ	function	temp, °C	a_1	a_2	a_3	a_4	σ
					(A) Anisole (1)–Cyclohexane (2)								
V^E, cm³/mol	25	2.809	−0.245	0.384	2.259	0.080	$\bar{V}_2$, cm³/mol	25	3.456	0.706	1.088	0.430	0.098
	30	2.599	0.978	−0.542	−0.072	0.015		30	3.043	−0.042	−0.041	−0.012	0.003
	35	2.633	0.770	−0.195	0.411	0.041		35	3.220	0.191	0.222	0.073	0.018
	40	2.760	1.281	0.308	−0.450	0.019		40	3.684	0.299	−0.061	−0.126	0.022
η^E, cP	25	−0.607	−0.141	−0.037	−0.235	0.002	A_{12}	25	0.023	0.003	0.000		0.004
	30	−0.535	−0.143	−0.016	−0.199	0.002		30	0.021	0.005	−0.004		0.001
	35	−0.473	−0.131	0.008	−0.193	0.002		35	0.020	0.005	0.000		0.002
	40	−0.409	−0.124	0.015	−0.133	0.001		40	0.021	0.006	0.003		0.001
G^E, kcal/mol	25	−0.402	−0.133	−0.385	−0.123	0.001	$(\partial\rho/\partial\phi_1)_{P,T}$	25	0.215	−0.020	0.000		0.003
	30	−0.388	−0.138	0.004	−0.121	0.001		30	0.216	−0.016	−0.003		0.006
	35	−0.373	−0.139	0.021	−0.130	0.001		35	0.216	−0.018	−0.002		0.006
	40	−0.351	−0.139	0.028	−0.098	0.001		40	0.216	−0.019	−0.003		0.002
$\bar{V}_1$, cm³/mol	25	1.119	−1.516	0.281	−0.282	0.113							
	30	1.111	−0.959	0.234	−0.401	0.043							
	35	1.083	−1.074	0.254	−0.358	0.097							
	40	1.069	−1.049	0.355	−0.337	0.015							
					(B) Anisole (1)–Nitrobenzene (2)								
V^E, cm³/mol	25	−0.491	0.124	0.259	−0.359	0.012	$\bar{V}_2$, cm³/mol	25	−0.392	0.047	−0.118	−0.085	0.019
	30	−0.540	−0.010	−0.149	0.390	0.014		30	−0.500	0.033	0.157	0.083	0.020
	35	−0.522	0.067	−0.082	−0.061	0.022		35	−2.277	−1.614	−2.876	−1.225	0.030
	40	−0.467	0.307	−0.323	−0.990	0.016		40	−0.673	−0.332	−0.489	−0.191	0.050
η^E, cP	25	−0.474	−0.118	0.134	−0.063	0.002	A_{12}	25	−0.005	−0.001	0.002		0.001
	30	−0.413	−0.124	0.154	0.015	0.005		30	−0.006	0.001	−0.001		0.001
	35	−0.368	−0.097	0.139	−0.013	0.004		35	−0.005	−0.001	0.000		0.002
	40	−0.319	−0.081	0.149	−0.004	0.004		40	−0.005	−0.003	−0.005		0.002
G^E, kcal/mol	25	−0.100	−0.006	0.079	−0.065	0.009	$(\partial\rho/\partial\phi_1)_{P,T}$	25	−0.210	0.004	0.002		0.001
	30	−0.094	−0.019	0.090	−0.026	0.003		30	−0.209	0.007	−0.001		0.001
	35	−0.093	−0.011	0.090	−0.043	0.003		35	−0.209	0.006	0.002		0.001
	40	−0.085	−0.008	0.099	−0.048	0.003		40	−0.209	0.007	0.004		0.001
$\bar{V}_1$, cm³/mol	25	−0.250	0.252	−0.028	0.088	0.050							
	30	−0.268	0.295	−0.145	0.068	0.030							
	35	0.282	0.193	0.564	−0.100	0.070							
	40	−0.150	0.353	−0.046	−0.006	0.120							
					(C) Anisole (1)–1,2-Dichloroethane (2)								
V^E, cm³/mol	25	0.794	−0.035	0.189	0.433	0.006	$\bar{V}_2$, cm³/mol	25	0.976	0.188	0.224	0.074	0.020
	30	0.848	0.387	−0.030	−0.397	0.011		30	0.997	−0.034	−0.158	−0.083	0.020
	35	0.757	−0.164	0.435	0.410	0.018		35	0.949	0.261	0.242	0.064	0.020
	40	0.926	0.329	0.222	−0.589	0.013		40	1.429	0.323	0.330	0.096	0.020
η^E, cP	25	−0.117	−0.011	0.242	0.001	0.003	A_{12}	25	0.010	0.002	0.002		0.001
	30	−0.106	−0.026	0.228	−0.003	0.003		30	0.011	0.002	−0.002		0.001
	35	−0.087	0.003	0.208	−0.015	0.002		35	0.009	0.000	0.006		0.001
	40	−0.071	−0.016	0.178	0.010	0.003		40	0.011	0.001	0.004		0.002
G^E, kcal/mol	25	−0.030	−0.015	0.166	0.030	0.002	$(\partial\rho/\partial\phi_1)_{P,T}$	25	−0.261	−0.026	−0.009		0.018
	30	−0.030	−0.022	0.167	0.019	0.002		30	−0.253	−0.011	−0.004		0.001
	35	−0.023	−0.002	0.171	0.012	0.002		35	−0.250	−0.013	−0.001		0.001
	40	−0.015	−0.015	0.157	0.025	0.002		40	−0.248	−0.014	−0.002		0.001
$\bar{V}_1$, cm³/mol	25	0.318	−0.431	0.110	−0.072	0.067							
	30	0.367	−0.314	0.123	−0.126	0.030							
	35	0.297	−0.481	0.151	−0.043	0.065							
	40	0.298	−0.386	0.069	−0.077	0.083							
					(D) Anisole (1)–Chlorobenzene (2)								
V^E, cm³/mol	25	0.040	−0.128	−0.189	0.310	0.020	$\bar{V}_2$, cm³/mol	25	−0.044	−0.030	0.104	0.070	0.015
	30	0.070	0.200	−0.249	−0.080	0.017		30	−0.048	−0.126	−0.074	−0.005	0.003
	35	0.050	−0.287	−0.107	0.936	0.013		35	0.068	0.134	0.395	0.193	0.042
	40	−0.012	−0.142	0.295	0.733	0.042		40	0.228	0.290	0.371	0.130	0.032
η^E, cP	25	0.042	0.003	0.176	−0.065	0.003	A_{12}	25	0.001	0.000	−0.004		0.002
	30	0.039	0.001	0.174	−0.048	0.004		30	0.001	0.002	−0.004		0.001
	35	0.032	0.014	0.151	−0.081	0.003		35	0.001	0.001	−0.002		0.001
	40	0.044	0.006	0.138	−0.059	0.003		40	0.001	0.002	−0.003		0.003
G^E, kcal/mol	25	0.050	0.005	0.117	−0.021	0.002	$(\partial\rho/\partial\phi_1)_{P,T}$	25	−0.111	0.001	−0.001		0.001
	30	0.050	0.005	0.126	−0.014	0.003		30	−0.111	0.001	−0.002		0.001
	35	0.042	0.011	0.119	−0.040	0.002		35	−0.110	0.000	−0.002		0.001
	40	0.052	0.007	0.120	−0.029	0.037		40	−0.109	0.000	−0.003		0.001
$\bar{V}_1$, cm³/mol	25	0.035	−0.034	−0.030	−0.018	0.037							
	30	0.064	−0.002	−0.011	−0.039	0.008							
	35	0.003	−0.087	−0.065	−0.006	0.108							
	40	−0.079	−0.060	−0.028	−0.054	0.082							
					(E) Anisole (1)–Carbon Tetrachloride (2)								
V^E, cm³/mol	25	−0.210	0.154	0.027	0.085	0.012	η^E, cP	30	0.034	−0.085	0.193	0.048	0.004
	30	−0.272	0.264	−0.277	0.162	0.021		35	0.033	−0.068	0.132	−0.007	0.002
	35	0.934	0.066	−2.628	−0.049	0.097		40	0.033	−0.016	0.138	−0.099	0.003
	40	−0.159	0.009	−0.011	−0.270	0.017	G^E, kcal/mol	25	0.029	−0.049	0.095	−0.011	0.001
η^E, cP	25	0.041	−0.082	0.156	−0.025	0.002		30	0.026	−0.055	0.127	0.037	0.003

Table III (Continued)

function	temp, °C	a_1	a_2	a_3	a_4	σ
G^E, kcal/mol	35	0.034	−0.049	0.080	−0.003	0.002
	40	0.029	−0.012	0.110	−0.075	0.002
$\bar{V}_1$, cm³/mol	25	−0.136	0.153	−0.062	0.036	0.003
	30	−0.157	0.255	−0.129	0.015	0.008
	35	0.728	−0.158	−0.144	−0.412	0.020
	40	−0.098	0.090	−0.059	0.027	0.025
$\bar{V}_2$, cm³/mol	25	−0.063	0.067	0.053	0.011	0.004
	30	−0.157	−0.022	0.052	0.038	0.008
	35	−0.180	−1.151	−0.421	0.100	0.005
$\bar{V}_2$, cm³/mol	40	−0.078	0.068	0.125	0.054	0.012
A_{12}	25	−0.003	0.002	0.001		0.001
	30	−0.004	0.003	−0.001		0.002
	35	0.010	−0.001	−0.022		0.001
	40	−0.002	0.001	0.000		0.001
$(\partial\rho/\partial\phi_1)_{P,T}$	25	−0.596	0.003	−0.002		0.001
	30	−0.590	0.005	−0.003		0.001
	35	−0.585	0.001	−0.001		0.003
	40	0.581	0.002	0.000		0.001

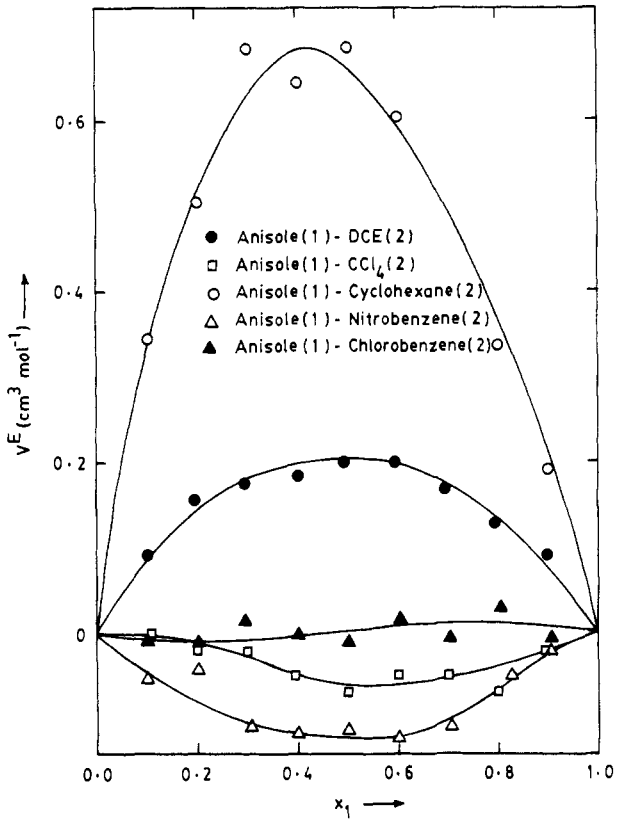

Figure 3. Variation of excess volume, V^E, with mole fraction at 25 °C. Symbols have the same meaning as in Figure 1.

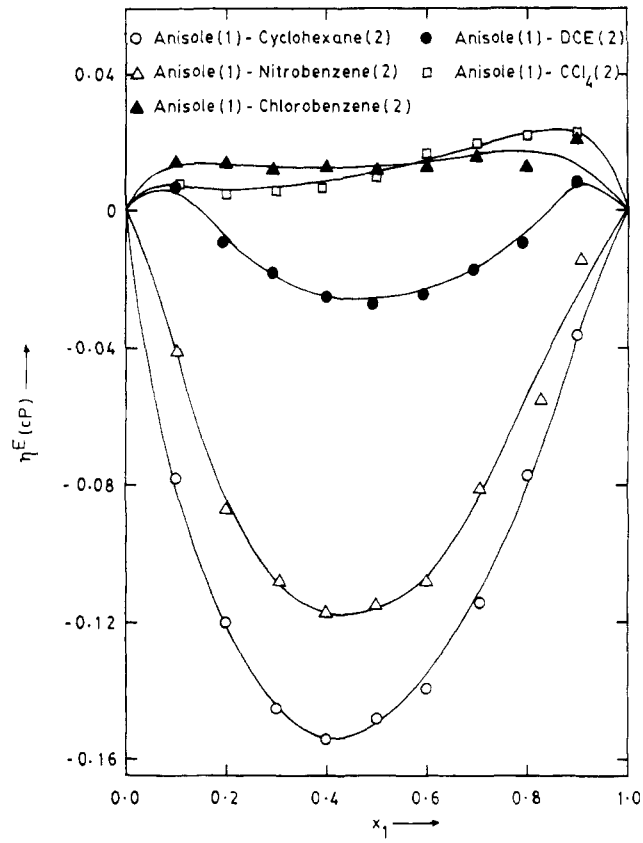

Figure 4. Variation of excess viscosity, η^E, with mole fraction at 25 °C. Symbols have the same meaning as in Figure 1.

The excess molar viscosity at 25 °C versus x_1 is displayed in Figure 4. The mixtures of anisole with cyclohexane exhibits the highest negative η^E (η^E_{max} = −0.154 cP) whereas, with nitrobenzene, it exhibits a less negative η^E (η^E_{max} = −0.117 cP). However, with anisole (1)–1,2-dichloroethane (2), a still negative η^E (η^E_{max} = −0.027 cP) is observed. Particularly for the latter mixture, η^E passes through a minimum, but it shows two maxima in the positive η^E scale (around x_1 = 0.1 or 0.9). Being a straight chain linear molecule, 1,2-dichloroethane might change its conformation due to free rotation around a C–C bond in solution, thereby producing both positive and negative values of η^E over the entire composition scale. Similarly, mixtures of anisole with either chlorobenzene or carbon tetrachloride behave almost in an identical manner as both the mixtures yield positive η^E and no sharp maxima are observed for these mixtures. However, sharp maxima in η^E vs x_1 plots are prevalent only with anisole (1)–cyclohexane (2) and anisole (1)–nitrobenzene (2) mixtures, suggesting the formation of molecular complexes in solution.

The dependence of excess molar Gibbs free energy, G^E, of activation of flow on x_1 is displayed in Figure 5. It may be noted that the curves for η^E and G^E are very much identical over the entire composition scale. For instance, the mixtures of anisole with chlorobenzene or carbon tetrachloride exhibit positive G^E with no clear-cut maxima. A flattened positive deviation of G^E with respect to mole fraction scale as shown by mixtures of anisole with chlorobenzene or carbon tetrachloride suggests the absence of molecular complexes in solution. This observation is further supported by the prevalence of small but negative values of V^E for these systems. The G^E curve for anisole (1)–carbon tetrachloride (2) system steadily increases with an increase in x_1, attaining the maximum at x_1 = 0.9. However, the G^E data for anisole (1)–dichloroethane (2) mixture shows a minimum in the negative scale and two maxima in the positive scale (one observed at x_1 = 0.1 and the other at x_1 = 0.9). This behavior is also identical with the η^E vs x_1 curve for this mixture. A sharp minimum with a large negative G^E (G^E = −104 cal/mol) is shown by the anisole (1)–cyclohexane (2) mixture, whereas a somewhat flattened minimum is observed for the anisole (1)–nitrobenzene (2) system. To the best of our knowledge, excess properties of the systems studied here are not available in the literature, and thus, no comparison of our data with literature findings could be attempted.

In Figure 6 the plots of $\bar{V}_1$ and $\bar{V}_2$ vs x_1 for some representative mixtures are given. It is observed that these dependencies are noticeable for the anisole (1)–cyclohexane (2) system as compared to the remaining mixtures. Figure 7 displays the variation of density increment on x_1 wherein linear dependencies are observed for mixtures of anisole with cyclohexane or DCE. On the other hand, for mixtures of anisole with

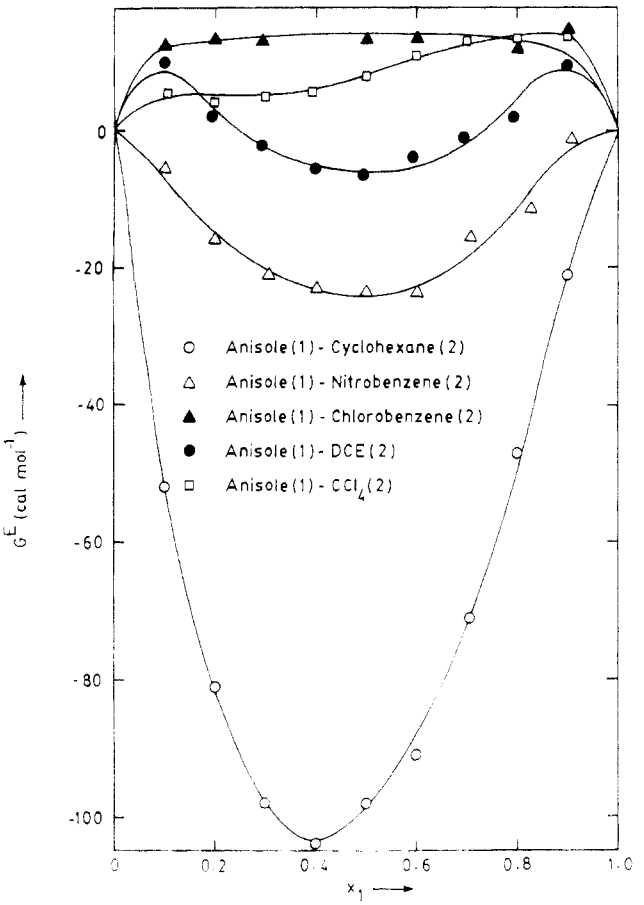

Figure 5. Variation of excess free energy of activation, G^E, with mole fraction at 25 °C. Symbols have the same meaning as in Figure 1.

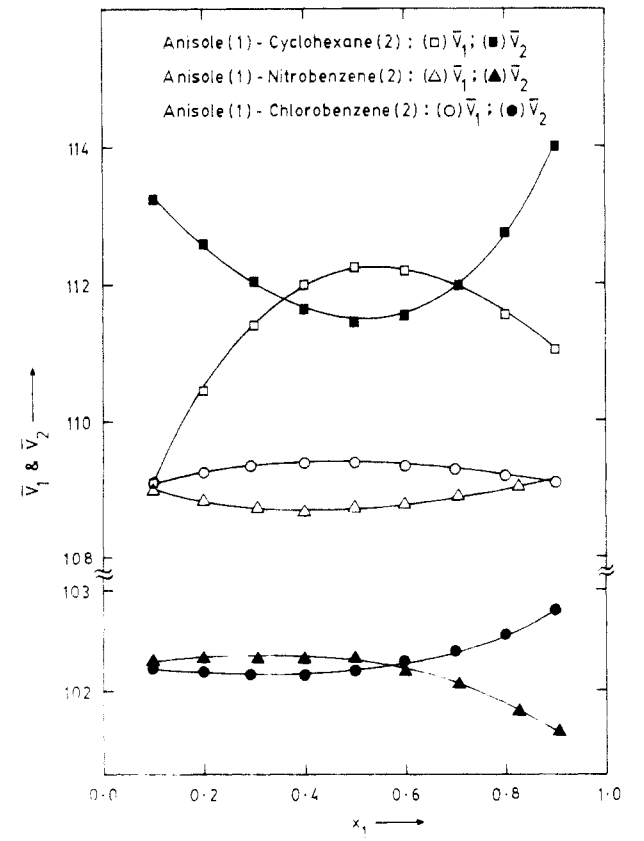

Figure 6. Variation of partial molar volumes with mole fraction at 25 °C for mixtures of anisole with (○) $\bar{V}_1$ and (●) $\bar{V}_2$ of chlorobenzene: (△) $\bar{V}_1$ and (▲) $\bar{V}_2$ of nitrobenzene; (□) $\bar{V}_1$ and (■) $\bar{V}_2$ of cyclohexane.

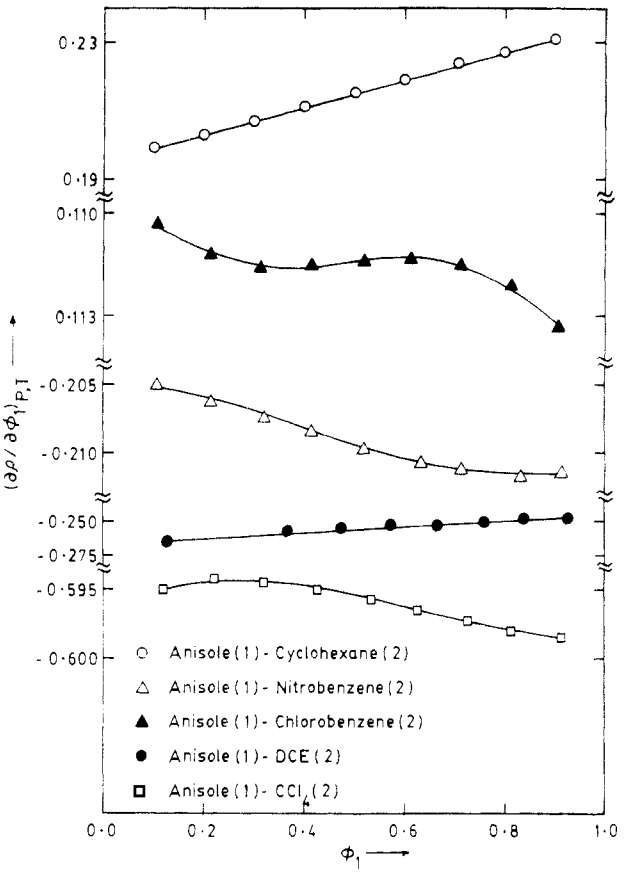

Figure 7. Variation of the density increment, $(\partial \rho/\partial \phi_1)_{P,T}$, with mole fraction at 25 °C. Symbols have the same meaning as in Figure 1.

nitrobenzene, chlorobenzene, and carbon tetrachloride, deviations from linearity are observed.

The values of ΔH^* as evaluated from eq 11 are positive, whereas ΔS^* are negative for all the binary mixtures. This suggests that the mixing is considered to be an endothermic process and the orderliness of the liquid structure is maintained while mixing. It is to be noted that ΔH^* values of all the mixtures vary in the range of 2–3 kcal/mol and the $-\Delta S^*$ values vary from 10–13 (cal/mol)/°C. However, both ΔH^* and $-\Delta S^*$ values do not seem to depend greatly on the mixture composition.

Analysis of viscosity data in terms of viscosity models suggests that the Heric relations, namely, eqs 13 and 14, seem to reproduce the experimental data within the average standard error σ of about 0.004, whereas McAllister theory (eq 12) reproduces the predicted data to experiments with a σ value of about 0.04. However, Auslaender theory (eq 15) showed an average σ value of about 0.007. This further suggests that, on a relative basis, Heric equations may be somewhat better than either Auslaender or McAllister equations in predicting the binary viscosity data.

Acknowledgment

We acknowledge Dr. Keith Hansen, Chairman, and Dr. John Idoux, Dean of Arts and Sciences, Lamar University, for their interest in establishing a mutual research program between Karnatak and Lamar Universities.

Registry No. Anisole, 100-66-3; nitrobenzene, 98-95-3; chlorobenzene, 108-90-7; carbon tetrachloride, 56-23-5; cyclohexane, 110-82-7; 1,2-dichloroethane, 107-06-2.

Literature Cited

(1) Manjeshwar, L. S.; Aminabhavi, T. M. *J. Chem. Eng. Data* **1987**, *32*, 409.

(2) Aminabhavi, T. M.; Manjeshwar, L. S.; Balundgi, R. H.; Halligudi, S. B. *Indian J. Chem.* **1988**, *27A*, 303.
(3) Aminabhavi, T. M.; Manjeshwar, L. S.; Halligudi, S. B.; Balundgi, R. H. *Indian J. Chem.* **1989**, *28A*, 217.
(4) McAllister, R. A. *AIChE J.* **1960**, *6*, 427.
(5) Heric, E. L. *J. Chem. Eng. Data* **1966**, *11*, 66.
(6) Heric, E. L.; Brewer, J. G. *J. Chem. Eng. Data* **1967**, *12*, 574.
(7) Ausiaender, G. *Br. Chem. Eng.* **1964**, *9*, 610.
(8) Riddick, J. A.; Bunger, W. B. *Organic Solvents*, 3rd ed.; Techniques in Chemistry, Vol. II; Wiley-Interscience: New York, 1970.
(9) Gokavi, G. S.; Raju, J. R.; Aminabhavi, T. M.; Balundgi, R. H.; Muddapur, M. V. *J. Chem. Eng. Data* **1988**, *31*, 15.
(10) Aminabhavi, T. M. *J. Chem. Eng. Data* **1987**, *32*, 406.
(11) Aminabhavi, T. M.; Munk, P. *Macromolecules* **1979**, *12*, 1186.
(12) Glasstone, S.; Laidler, K. J.; Eyring, H. *The Theory of Rate Processes*; McGraw-Hill: New York, 1941.

Received for review August 7, 1989. Accepted February 14, 1990. T.M.A. and S.S.J. are thankful to the University Grants Commission [F. 12-55/88-(SR-III)], New Delhi, India, for financial support of this study. S.S.S. and T.M.A. appreciate the partial support from the Robert A. Welch Foundation, Houston, TX.

Thermodynamics of the Dissociation of Boric Acid in Potassium Chloride Solutions from 273.15 to 318.15 K

Andrew G. Dickson

Marine Physical Laboratory, S-002, Scripps Institution of Oceanography, La Jolla, California 92093-0902

Electromotive force measurements have been made with the cell Pt|H_2(g, 101.325 kPa)|KCl (m_1),borax (m_2)|AgCl;Ag over the temperature range 273.15–318.15 K and at five ionic strengths from 0.1 to 1.5 mol·kg^{-1}. The results have been used to calculate the stoichiometric (ionic medium) dissociation constant for boric acid in potassium chloride media.

Introduction

A recent study by Felmy and Weare (*1*) has shown that the chemistry of boron in naturally occurring aqueous electrolyte solutions can be represented by a combination of chemical equilibria and ionic interactions. In the course of this work, Felmy and Weare identified the need for measurements that could be used to obtain parameters for the interaction of potassium ion with orthoborate ion.

The best technique available to characterize the extent of this interaction uses the cell

$$\text{Pt}|H_2(\text{g, 101.325 kPa})|\text{KCl } (m_1),\text{borax } (m_2)|\text{AgCl;Ag} \quad \text{(A)}$$

to make measurements at various concentrations of potassium chloride and of borax. This cell is similar to that used by Owen and King (*2*) to measure the dissociation constant of boric acid in sodium chloride media. I report here measurements on cell A over a range of ionic strengths and temperatures and at three values of m_2. In addition, these values have been used to calculate the ionic medium (stoichiometric) dissociation constants of boric acid in potassium chloride media. The interpretation of these results in terms of ionic interactions—Pitzer coefficients (*3*)—has been performed for the electromotive forces (emfs) at 298.15 K and reported elsewhere (*1*); further work extending the modeling of aqueous boron systems to a range of temperatures is currently in progress.

Experimental Section

The chemicals used in this work were of high purity. The borax was recrystallized from water, taking care to keep the temperature below 328 K (*4*). It was stored in a hygrostat (over a saturated solution of sucrose and sodium chloride) for a number of weeks to ensure the correct extent of hydration ($Na_2B_4O_7\cdot 10H_2O$) and then assayed by titration with hydrochloric acid, which in turn had been assayed as silver chloride (*5*). The potassium chloride (reagent grade) was recrystallized from water and dried at 575 K. All dilutions were carried out with ultrafiltered, deionized water (Milli-Q); all apparent masses were corrected to mass. The details of electrode preparation and cell design have been given elsewhere, together with a description of relevant experimental procedures (*6*). All emfs reported have been corrected to a hydrogen fugacity of 101.325 kPa (see footnote to Table I) and have been adjusted so that the values of E° correspond to those published by Bates and Bower (*7*). This was achieved by subtracting the difference

$$\Delta E^\circ/\text{V} = [E^\circ(298.15\text{ K})/\text{V}] - 0.22240 \quad (1)$$

from each emf reading. E°(298.15 K) was measured with cells containing hydrochloric acid at 0.01 mol·kg^{-1} (*6*, *8*, *9*). Typically ΔE° amounted to 0.000 02 V.

Results

Table I contains values for the corrected emfs of cell A from 273.15 to 318.15 K at potassium chloride concentrations of approximately 0.1, 0.3, 0.5, 1.0, and 1.5 mol·kg^{-1} and at borax molalities of 0.005, 0.01, and 0.015 mol·kg^{-1}. The exact values of m_1 and m_2 corresponding to these nominal values are given in the table.

When the salt borax is dissolved in water, it yields an equimolal mixture comprised of boric acid and sodium orthoborate:

$$Na_2B_4O_7\cdot 10H_2O = 2B(OH)_3 + 2Na^+ + 2B(OH)_4^- + 5H_2O \quad (2)$$

The charge-balance expression for the solution is thus

$$m(K^+) + m(Na^+) + m(H^+) = m(Cl^-) + m(B(OH)_4^-) + m(OH^-) \quad (3)$$

and hence

$$m(B(OH)_4^-) = 2m_2 - m(OH^-) + m(H^+) \quad (4)$$

where m_2 is the molality of borax. The mass balance equation for boron is

$$4m_2 = m(B(OH)_3) + m(B(OH)_4^-) \quad (5)$$

Substituting in eq 4 gives

$$m(B(OH)_3) = 2m_2 + m(OH^-) - m(H^+) \quad (6)$$

0021-9568/90/1735-0253$02.50/0